JOURNAL OF PROPULSION AND POWER
Vol. 23, No. 2, March–April 2007

Direct Experimental Evidence of Electromagnetic Inertia Manipulation Thrusting

Hector H. Brito*
Instituto Universitario Aeronautico, 5010 Cordoba, Argentina
and
Sergio A. Elaskar†
CONICET, Universidad Nacional de Cordoba, 5000 Cordoba, Argentina

DOI: 10.2514/1.18897

New experimental results suggesting that "propellantless" propulsion without conventional external assistance has been achieved by means of electromagnetic inertia manipulation are discussed here and compared with previous work along the same line of research. The underlying theory, based on Minkowski's energy–momentum tensor for describing field–matter interactions and justifying that the inertial properties of the field-generating device can be modified, is revisited. Former tests of an electromagnetic inertia manipulation thruster, engineered up to the "proof of concept" level, having yielded increasingly sharper and clearer evidence of alternate, later sustained thrusting, are briefly discussed. Recent testing activities, where increased power, improved power processing strategy, and optimal use of the sensing device sensitivity were applied, resulted in a direct thrust signal, as observable in time domain plots. These results, on the basis of a reassessment of uncertainties, are shown to be consistent with an alternative formulation of Minkowski's electromagnetic force density, which correctly predicts related peer-reviewed experimental results.

Nomenclature

$\boldsymbol{B}$	=	magnetic induction vector, T
c_0	=	velocity of light in vacuum, m/s
D	=	width of the annular capacitor, m
$\boldsymbol{D}$	=	electric displacement vector, C/m^2
D/Dt	=	material derivative with respect to time
E	=	electric field intensity, N/C
$\boldsymbol{E}$	=	electric field vector, N/C
$\boldsymbol{f}$	=	electromagnetic force density, N/m^3
$\boldsymbol{G}$	=	total electromagnetic momentum, N · s
$\boldsymbol{g}$	=	electromagnetic momentum density, N · s/m^3
H	=	magnetic field intensity, A/m
$\boldsymbol{H}$	=	magnetic field vector, A/m
I	=	electric current, A
$\boldsymbol{J}$	=	electric current density, A/m^2
n	=	number of turns of the toroidal coil
$\boldsymbol{n}$	=	normal unit vector
S	=	area, m^2
$\boldsymbol{s}$	=	energy flow, W/m^2
T	=	thrust intensity, N
$\boldsymbol{T}$	=	thrust vector, N
t	=	time, s
V	=	voltage, V; volume, m^3
$\boldsymbol{v}$	=	velocity vector, m/s
w	=	energy density, J/m^3
$\boldsymbol{x}$	=	position vector, m
ε	=	permittivity of the medium, F/m
μ	=	magnetic permeability, H/m
ρ	=	density of charge, C/m^3
φ	=	relative phase angle of current and voltage, rad
ψ	=	angle between ground and thruster reference frames, rad
ω	=	angular frequency, rad/s

Subscripts

F	=	related to fields in matter
r	=	relative

Superscripts

A	=	related to Abraham
f	=	field
M	=	related to Minkowski
m	=	matter

Presented as Paper 4989 at the 39th AIAA/ASME/SAE/ASEE Joint Propulsion Conference and Exhibit, Huntsville, AL, 20–23 July 2003; received 17 July 2005; revision received 14 June 2006; accepted for publication 25 June 2006.

*Program Manager, Space Vehicles Department, Ruta 20, Kilometer 5.5. Senior Member AIAA.

†Associate Professor, Department of Aeronautics, Avenue Velez Sarfield 1601.

I. Introduction

EITHER for going to the stars or, more pragmatically, to substantially cut down space transportation costs, new propulsion mechanisms must be found which get rid of propellants and/or conventional external assistance, i.e., the mythical "space drive" must still be invented [1].

Recent theoretical works show that jetless-sailless-beamless-tetherless propulsion can be achieved by manipulating the spaceship inertia in a way analogous to a dancer who increases her angular velocity by manipulating her body moment of inertia. The analogy goes this way: by considering space-time instead of three-space, the spaceship four-velocity (angular velocity analog) can be changed by manipulating its mass tensor components (moment of inertia tensor analog). To do that, an "extended" spaceship including the fields it eventually generates must be considered; a thrust then appears on the "material" spaceship by means of momentum exchange with its "field" counterpart by virtue of the four-momentum conservation law. It is shown that the physical signature of a nondiagonal mass tensor is the existence of a nonvanishing linear momentum in the spaceship rest frame [2,3].

When the electromagnetic (EM) field is chosen as the field counterpart, one may wonder if a static EM momentum can develop in the rest frame of the material spaceship. A possibility arises from a

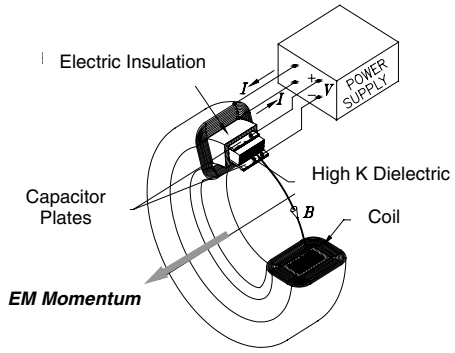

Fig. 1 Electromagnetic momentum generator schematics.

physical arrangement of electric and magnetic sources including polarizable media, as depicted in Fig. 1. Different theoretical results are possible depending on whether Planck's principle of inertia of the energy is satisfied or not between the Poynting vector (energy flow density) and the EM momentum density [4]. The results are basically Abraham's and Minkowski's forms of the EM momentum density, three-dimensional expressions of the so-called Abraham–Minkowski controversy about the correct energy-momentum tensor of EM fields in polarizable media. The controversy, lasting since 1909, strikingly remains as a yet unsolved issue of physics [5,6], with existing experimental evidence not yet allowing drawing definite conclusions.

By Minkowski's formalism, a nonvanishing momentum of electromagnetic origin is shown to arise for the particular device depicted in Fig. 1 [7–9]. It follows that the EM field can modify the inertial properties of the generating device, their variation producing forces on the device without any exchange of mass-energy with the surrounding medium. A propulsion concept based upon this kind of inertia manipulation mechanism was subsequently drawn; an electromagnetic inertia manipulation (EMIM) thruster was engineered up to the "proof of concept" level. Experiments were designed and performed, yielding by spectral analysis techniques, in an exploratory phase, indirect evidence of Minkowski's approach being valid. In a second phase, with a slightly modified experiment, sharper and clearer evidence of sustained thrust has been found, as observed in frequency domain plots, too [3,10,11]. This paper aims at presenting additional experimental work by the authors, where direct evidence of EMIM sustained thrust seems to emerge from the obtained results. These are compared with theoretical predictions and experimental results recently reported by another research team using a slightly different thrusting device, although having the same configurational concept as the authors' [12].

II. Theoretical Background

A. EM Field Momentum Approach

The device depicted in Fig. 1 bears an EM momentum density distribution in its rest "matter" frame, i.e., in the frame comoving with the hardware when all EM fields are off. This comes directly out from the particular electric and magnetic fields distribution, namely, "crossed" fields, which enter the following mathematical expression of the EM momentum density:

Abraham's claim:

$$\boldsymbol{g}^{A} = \frac{(\boldsymbol{E} \times \boldsymbol{H})}{c_0^2} \tag{1}$$

Minkowski's claim:

$$\boldsymbol{g}^{M} = (\boldsymbol{D} \times \boldsymbol{B}) \tag{2}$$

Abraham's expression is fully consistent with Planck's principle of inertia, because $\boldsymbol{E} \times \boldsymbol{H}$ represents the EM energy flow, whereas Minkowski's is not. Equations (1) and (2) are the vector expressions of the still-standing Abraham–Minkowski controversy about the form of the electromagnetic energy-momentum tensor, especially for low frequency or quasi-stationary fields [4,13–15]. The question arises whether these nonzero EM momentum densities can lead to a nonzero total EM momentum. It can be shown that for any closed matter–field configuration, provided the fields die out rapidly at infinity [16] or nullify at the boundary, the total EM momentum in any frame can be written as

$$\boldsymbol{G}^{(f)} = \int_V \boldsymbol{g}^{(f)}\,\mathrm{d}V = -\int_V \boldsymbol{x}\left[\operatorname{grad}\left(\frac{1}{c_F^2}\right)\cdot \boldsymbol{s}^{(f)} + \left(\frac{1}{c_F^2}\right)\operatorname{div}\boldsymbol{s}^{(f)}\right]\mathrm{d}V \tag{3}$$

$c_F = c_0$ in Abraham's formulation, whereas $c_F = c$, velocity of light in the medium in Minkowski's formulation.

The quantity between brackets being $\operatorname{div}\boldsymbol{g}^{(f)}$, a nonzero LHS is possible provided $\boldsymbol{g}^{(f)}$ is not divergence-free everywhere. This can be achieved for arbitrary matter–field configurations if gradients of the dielectric and/or magnetic properties of the medium occur in the region of integration and enter the formulation, i.e., if Minkowski's formulation is adopted. This is the case for the setup shown in Fig. 2, where $\operatorname{div}\boldsymbol{s}^{(f)} = 0$ everywhere, and a nonvanishing total EM momentum can only arise from the RHS first term of Eq. (3). The contributions for the volume integral come from the free surfaces of the dielectric, through which jumps of the velocity of light hold in the direction of the EM energy flux.

Because for closed systems the Law of Momentum Conservation implies

$$\int_V (\boldsymbol{g}^{(m)} + \boldsymbol{g}^{(f)})\,\mathrm{d}V = \text{const} \tag{4}$$

it follows when the integration volume is restricted to be a material one comprising the spaceship's matter

$$\frac{\mathrm{D}}{\mathrm{D}t}\int_{V_m} \boldsymbol{g}^{(m)}\,\mathrm{d}V = -\frac{\mathrm{D}}{\mathrm{D}t}\int_{V_m} \boldsymbol{g}^{(f)}\,\mathrm{d}V \tag{5}$$

Therefore, the LHS of Eq. (5) is the total force acting upon the system matter, i.e., the *thrust*. As previously seen, this thrust can amount to something different from zero provided Minkowski's expression for the EM momentum density is applied. As for the RHS of Eq. (5), it can generally be expressed as (Reynold's Transport Theorem)

$$\frac{\mathrm{D}}{\mathrm{D}t}\int_{V_m} \boldsymbol{g}^{(f)}\,\mathrm{d}V = \int_{V_m}\left[\frac{\partial \boldsymbol{g}^{(f)}}{\partial t} + \operatorname{div}(\boldsymbol{g}^{(f)} \otimes \boldsymbol{v})\right]\mathrm{d}V \tag{6}$$

Thus, the following general expression for the electromagnetic thrust on closed systems can be derived:

$$\boldsymbol{T} = -\int_{V_m} \frac{\partial \boldsymbol{g}^{(f)}}{\partial t}\,\mathrm{d}V - \int_{\partial V_M} \boldsymbol{g}^{(f)} \otimes \boldsymbol{v}\cdot\boldsymbol{n}\,\mathrm{d}S \tag{7}$$

Because the EM momentum densities are assumed to be negligible outside the material boundaries (besides a tiny radiation field), the

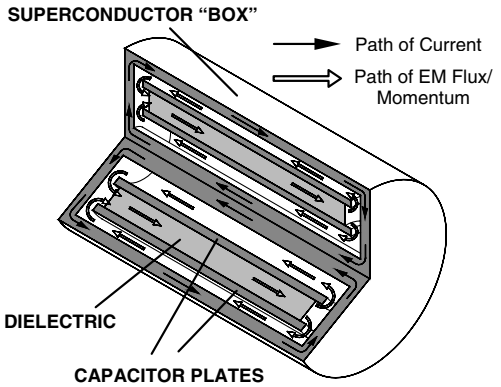

Fig. 2 Stationary regime in the "matter" rest frame with polarizable media.

RHS of Eq. (7) reduces to the first term. This is strictly true when the medium is at rest in the observer's frame. For practical purposes,

$$\boldsymbol{T} \cong -\int_{V_m} \frac{\partial \boldsymbol{g}^{(f)}}{\partial t}\,\mathrm{d}V = -\int_{V_m} \frac{\partial}{\partial t}(\boldsymbol{D}\times\boldsymbol{B})\,\mathrm{d}V \tag{8}$$

According to Eq. (8), EM inertia manipulation becomes a theoretical possibility. A positive answer concerning Minkowski's formulation would thus allow for "jetless" propulsive effects by means of EM fields manipulation.

B. EM Force Density Approach

There is an another variant of the Abraham–Minkowski controversy, this time in terms of force densities. If dispersion is negligible and the medium is allowed to be isotropic but spatially inhomogeneous, $\boldsymbol{D} = \varepsilon\boldsymbol{E}$, $\boldsymbol{B} = \mu\boldsymbol{H}$. The force densities are given by [4,10]

$$\boldsymbol{f}^{M} = \rho\boldsymbol{E} + \boldsymbol{j}\times\boldsymbol{B} - \frac{1}{2}E^2\nabla\varepsilon - \frac{1}{2}H^2\nabla\mu \tag{9}$$

$$\boldsymbol{f}^{A} = \boldsymbol{f}^{M} + \frac{\varepsilon_r\mu_r - 1}{c_0^2}\frac{\partial}{\partial t}(\boldsymbol{E}\times\boldsymbol{H}) \tag{10}$$

where the first two terms of Eq. (9) represent the Lorentz force density. These force densities clearly differ inside matter for generic fields; they are identical for static fields irrespective of the medium. If harmonic fields are considered, the force densities' instantaneous values differ, but their averaged values become identical and therefore useless for discriminating between the two formulations. This is the reason Walker and Walker's claim [17], favoring Abraham's one, is essentially wrong and their experiment remains inconclusive.

When application is made to the device of Fig. 1, with both $\boldsymbol{D}$ and $\boldsymbol{B}$ fields subjected to harmonic evolution, Eq. (9) can be used for its theoretical estimation, where only free charges and currents must be considered according to the "standard" treatment. As a result, nonzero instantaneous EM thrust is found albeit with zero time average. The same conclusion applies to Walker and Walker's experiment where torques rather than linear thrusts are involved. However, the measured time-averaged torques were different from zero, which was interpreted by the authors in terms of the polarization current contribution to the Lorentz force. James's experiment involved linear thrusts with both fields also subjected to harmonic evolution and the published results seemed to favor Abraham's formulation [18]. However, both experiments were recently analyzed by Obukhov and Hehl [19], finding the experimental results consistent with that corrected Lorentz force definition, instead of Eqs. (9) and (10).

Now, by assuming that the polarization current in the dielectric contributes the second term of the equation, the following expression for the EM average thrust on a closed system, as a function of the harmonic voltage $V\sin\omega t$ on the capacitor and the harmonic current $I\sin(\omega t + \varphi)$ on the coil, is found [10,11]:

$$\langle T\rangle = \frac{\varepsilon_r\varpi nIVd}{2c_0^2}\sin\varphi \tag{11}$$

From a phenomenological viewpoint, it can be seen that for this particular closed system the volume contribution of the Lorentz force density amounts to zero for the electrical part and nearly to zero for the magnetic part. Induced electric fields are perpendicular to the capacitor plates, whereas the self interaction between closed current loops (by including the polarization current across the dielectric) practically cancels out. The volume contribution of the gradient terms is left, which amounts to a nonzero instantaneous value due to the induced electric fields at the dielectric/vacuum interfaces, with a time average again given by Eq. (11). In summary, nonzero time average thrusts are somehow related to the existence conditions for the total EM momentum as stated in Sec. II.A, when the polarization currents are included in the magnetic self-interaction calculation.

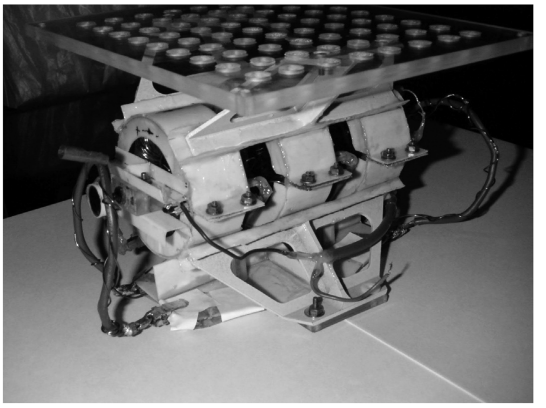

Fig. 3 EMIM thruster.

However, Eq. (11) must be seen as a conflicting result regarding momentum conservation. In fact, the standard treatment of the problem requires the polarization current to be excluded from the magnetic contribution to the Lorentz force, so the averaged thrust cancels out. Therefore, thrust experiments involving harmonic fields in a closed system should allow to discriminate between the standard and the "proposed" formulation.

III. Sustained Thrust Experiments: 1

Description and results of experiments geared to obtain sustained (or "rectified") EMIM propulsive effects, were previously detailed elsewhere [3,10,11]. The core device is shown in Fig. 3 and a summary of the relevant aspects is reproduced here for better understanding of new operating procedures and the resulting experimental data.

A. Experimental Setup Rationale

The experimental setup basically consists of mounting the device as a seismic mass atop a thin vertical cantilever beam (a resonant blade), sitting on a vibration-free platform. Piezoceramic strain transducers (PZTs) are used to detect the seismic mass displacements through output voltages proportional to the strain level in a broad dynamic range, achieving sensitivities up to 10^{-11} m/m [20]. The transducer analog output signal is digitalized for further processing through a 12 bit data acquisition board, making it available to PC-based storage devices. Sustained thrust experiments were implemented to get rid of previously observed interfering effects considered potential sources of uncertainties. A schematic view of the sensing concept is shown in Fig. 4.

A nonzero averaged (sustained) thrust was sought after in virtue of Eq. (11) by applying power to the electromagnetic momentum generator (EMMG) so that $\boldsymbol{D}$ and $\boldsymbol{B}$ fields were subjected to harmonic evolution with a variable phase shift. To take advantage of the sensing device characteristics, the polarity of the voltage amplitude is switched at a frequency different from the ac supply frequency which enters Eq. (11) as ϖ, so the seismic setup is set into

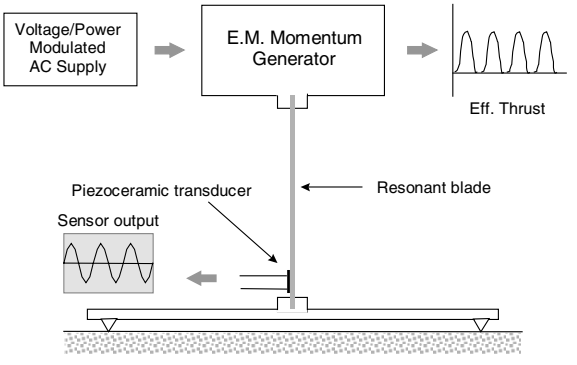

Fig. 4 Micromotion sensing concept.

vibratory motion if the "proposed" formulation is correct. By detecting this force, the geomagnetic influence becomes averaged out; direct detection in frequency domain also permits to get rid of numerical artifacts because advanced numerical filtering is no longer required; if the voltage amplitude switching frequency is different from the setup natural frequencies, ground noise becomes less significant. Air motion, being related to the power supply frequency, averages out too. Uncertainties were expected to remain regarding power supply induced EMI.

B. Setup Operation Rationale

A separate supply of 100 V ac at 30 kHz, to three 900 turns parallel mounted toroidal coils and to three parallel mounted 10 nF, 8 mm wide annular capacitors, allows for a total EM momentum (Minkowski's formulation) of around 50 $\mathrm{pN}\cdot\mathrm{s}$ (peak), by using $BaTiO_3$ ceramic dielectrics ($\varepsilon_r \approx 4400$). A maximum average thrust of around 5 μN should be obtained according to Eq. (11). A switching frequency of 30 Hz was chosen. Propulsive effects should show up only when the Caps ON–Coils ON condition holds, with a magnitude depending on the set voltage-current phase shift.

C. "Open System" Configuration Results

The hardware configuration with the device atop the resonant blade and external power supply was adopted for this test series. "Thrust OFF" and Thrust ON" conditions clearly yield different responses in the frequency domain. Phase shift dependence was investigated for power spectral density (PSD) peak values at 27 Hz and maxima of the alleged propulsive effect were obtained for a voltage-current phase shift of 90 deg, as predicted by the proposed formulation. Spreading of the PSD peak values was observed, their source remaining unknown except for fluctuations of ground noise components at the reversing frequency. Nevertheless, a slightly shifted squared sine trend is clearly seen to emerge from data.

D. "Closed System" Configuration Results

The hardware configuration was modified so the device could be operated in a full "closed system" mode. Both the EMMG and its power processing unit (PPU), including a 12 V, 1.2 Ah battery, were located and rigidly assembled atop the resonant blade of the sensing fixture. This would allow assessing the influence of external wiring on the previous test series. However, due to the added seismic mass, the thrust stand dynamics was considerably altered and only qualitative analyses could be done. Fully quantitative assessments demand a thoroughly thrust stand characterization, which is currently underway [21].

Data were processed in the frequency domain, too. To assess the influence of the switching frequency, tests were carried out at 32 and 38 Hz. Runs of cases "Thrust OFF" and "Coils ON–Caps OFF" behaved as expected, qualitatively similar to the corresponding "Open System" series data. Sharp spectral peaks show up in case "Thrust ON" runs, but, unexpectedly, spectral peaks show up in case "Caps ON–Coils OFF" runs, too, amounting to comparable order of magnitudes regarding "Thrust ON" type peaks. This effect is likely due to the vibratory motion, at the switching frequency, of a transformer casing in the secondary circuit of the capacitors supply line. Relative phase shift dependence at 32 Hz, taking into account the average peak values under "Caps ON–Coils OFF" conditions were found to fit a squared-sine law, with maxima at 90 deg, too.

IV. Sustained Thrust Experiments: 2

A. Experimental Setup

All components were kept without change, except for the EMMG, where the coils and capacitors banks were connected as an LC (inductor–capacitor) resonant circuit, and the PPU, which was redesigned to deliver higher power output than the one previously used, with a unique output line connected to that LC arrangement.

Power is applied to the EMMG so that $\boldsymbol{D}$ and $\boldsymbol{B}$ fields are subjected to harmonic evolution, this time with a fixed 90 deg phase shift, and a nonzero averaged (sustained) thrust was sought after in virtue of Eq. (11). To take advantage of the sensing device characteristics, the PPU output voltage supply is amplitude modulated following a sine law (instead of a square wave), at a frequency different from the supply frequency, so the seismic setup is set into vibratory motion if the proposed formulation is correct. Same considerations as under the previous heading apply regarding the uncertainties due to the expected interferences, although the new modulation procedure was thought to have a beneficial effect by minimizing power supply induced EMI in the PZT measurement line.

B. Modified Setup Operation

A common supply of 200 V ac at 39 kHz, to three 900 turns parallel mounted toroidal coils in series with three parallel mounted 10 nF, 8 mm wide annular capacitors, allows for a total Minkowski's EM momentum of around 100 $\mathrm{pN}\cdot\mathrm{s}$ (peak), by using $BaTiO_3$ ceramic dielectrics ($\varepsilon_r \approx 4400$). An average thrust of 13 μN should be obtained according to Eq. (11), for $\varphi = 90$ deg. Propulsive effects should show up only when the PPU-ON condition holds, with a magnitude depending on the modulation frequency, because the voltage-current phase shift is a built-in property of the LC resonant circuit.

The use of sine modulation of the supply ("carrier") voltage yields, when Eq. (11) is applied, a modulated average thrust, at the modulation and twice the modulation frequencies, with amplitudes $1/2$ and $1/8$, respectively, of the nonmodulated average thrust. This is a thrust model related feature and can be seen as the spectral signature of a sustained EMIM thrust. Because other EM coupling effects can show similar spectra order of magnitude estimates must be done to rule them out.

C. "Open System" Configuration Results

The device is atop the resonant blade with an external power supply. A comparison between "Thrust OFF" and Thrust ON" conditions is shown in Fig. 5. A comparison of "Thrust ON" results with the corresponding simulation results is shown in Fig. 6, where a good agreement is found for the response to the alleged EMIM averaged force at 27 Hz modulation frequency. The response at twice that frequency is underpredicted. Dependence on this parameter was

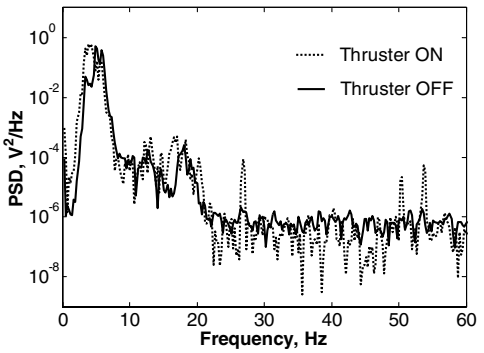

Fig. 5 PSD of thrust effect at 27 Hz.

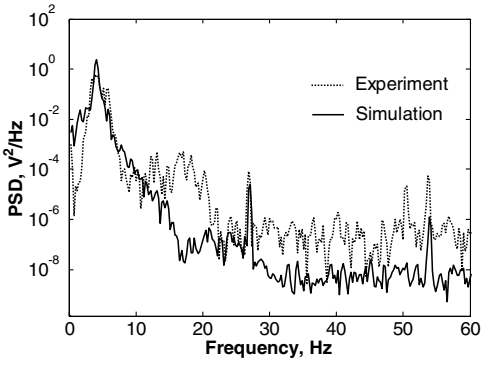

Fig. 6 PSD of "Thrust ON" experimental and simulation results.

investigated, but the useful range stretched between 25 Hz, the minimum modulation frequency outside the noisiest region of the spectrum, and 30 Hz, the maximum available modulation frequency. No conclusive results could be obtained because of very widespread experimental PSD peak values for a given modulation frequency were observed.

Spreading of the PSD peak values for a given frequency are thought to be related to temperature effect on the capacitors causing changes of capacitance, slight modulation frequency shifts to/from structure natural frequencies, or variable battery loading conditions. Their source remains unknown, except for fluctuations of ground noise components at the modulation frequency, as under the preceding heading.

D. "Closed System" Configuration Results

The hardware was configured for full "closed system" mode of operation. Both the EMMG and its redesigned PPU were located and rigidly assembled atop the resonant blade of the sensing fixture. Two 12 V, 1.2 Ah batteries were used instead of a single one. As a result, the total seismic mass is higher than for previous experiments and the first natural frequency of the thrust stand dynamics decreases to 1 Hz. This happens to have a beneficial effect on the vibration isolation characteristics of the whole experimental setup. The residual ground induced motion at the thrust stand base is considerably reduced with respect to former levels; the expected sensing device response to EMIM activation can now widely overcome the response to ground induced motion. A modulation frequency of 1 Hz was then selected, taking advantage of the mechanical amplification factor at resonance. Data were processed in the frequency domain for monitoring purposes, whereas time domain values were taken as the main experimental results. The PZT conditioned signal was also filtered using sharp low-pass finite impulse response (FIR) filters with a cutoff frequency at 1.5 Hz. A comparison between "Thrust OFF" (filtered) and Thrust ON" (raw and filtered) response signals is shown in Fig. 7.

1. *Reassessment of Uncertainties*

Although "Open System" sustained thrust experiments were found to get rid of most of the aforementioned interfering effects, "Closed System" versions of those experiments make appear potential sources of uncertaintities (spurious signals), such as [22] 1) electrostatic coupling to surroundings, 2) magnetic coupling to surroundings, 3) self-magnetic couplings, 4) air motion, 5) radiometer effects, 6) ground motion, 7) power supply induced EMI, 8) geomagnetic influence, and 9) thermal expansion due to Joule heating, which need to be addressed to assess their contribution when interpreting the results obtained in time domain in terms of EMIM propulsive effects.

2. *Electrostatic Coupling to Surroundings*

Alternating electric fields can be significant around the power wires of the EMIM device, where voltage alternates between +200 and −200 V. Alternating polarization in close-by conductors and insulators can thus be induced. The polarization in insulators can interact directly with the electric fields produced by the power wiring through the action of induced dipoles on the electric charges that create the field that induces the dipoles. When the voltage and electric charges change sign, the induced voltage will reverse orientation so the interaction can create a force that always acts in the same direction on mobile components of the setup, notwithstanding that the electric fields and induced dipoles time average to zero. Rough but very conservative estimates show that their contribution is two orders of magnitude lower than the observed effect.

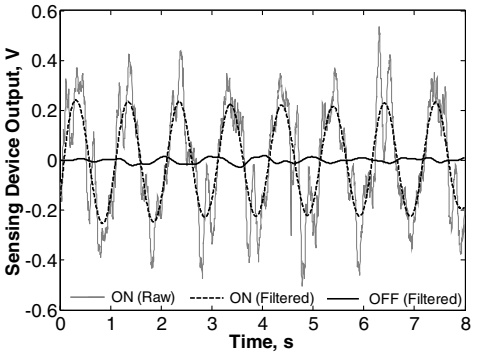

Fig. 7 Sensing device response to EMIM activation.

Static electric fields due to static electric charges in the surroundings cannot show any effect on static electric charges in the mobile parts of the setup, because PZTs are only sensitive to variable strains (unless special provisions are taken). The situation is in principle different when alternating electric charges in the mobile part are considered. Alternating forces develop that could produce some high frequency component on the PZT output, but having zero time average, their contribution at the modulation frequency cancels out, too.

3. *Magnetic Coupling to Surroundings*

Eddy currents in nearby conductors can also be induced by alternating electric fields, which can in turn interact magnetically with currents in the power circuitry of the device. In a way similar to the self-rectifying electrostatic interaction, these forces might induce torques on the sensing device. For this reason, the presence of conductors near that circuitry is minimized and, when present, they are made of nonferromagnetic materials. Again, rough and very conservative estimates show that their contribution is three orders of magnitude lower than the observed effect.

4. *Self-Magnetic Interaction*

Self-magnetic interactions in wiring and windings of PPU and EMMG components were also identified as an important potential source of mechanical noise. "Closed System" configuration means that all related current paths must also be closed, belonging then to the whole seismic (or mobile) mass of the thrust stand. If rigid wires and fixations are assumed, no unbalanced force should arise so there would be no contribution to the observed effect. On the contrary, if parts of the circuits are flexible and/or loosely fixed to the casing, inner relative motion will develop under the effect of magnetic forces due to the rest of the circuits. It can be shown that this interaction has a self-rectifying component acting in the same direction on the seismic mass of the setup. Rough but very conservative estimates show that their contribution for flexible wire segments is several orders of magnitude lower than the observed effect, but can amount to about the same order of magnitude for a transformer ferrite casing in the PPU's secondary circuit.

5. *Air Motion*

Three sources of interference have been considered: 1) gradient (thermal, pressure) forced airflow, 2) voltage gradient induced airflow (electric wind), and 3) sonic wind. Type 1 sources are present even in controlled room environment, although it is highly unlikely that they could bear an oscillatory behavior such as aerodynamic forces act upon the device with the right frequency. Type 2 interferences are known to be proportional to voltage differences between conductors in partially conducting media [23–25]; the voltage being subjected to harmonic evolution, they average out to zero. Sonic wind arises from nonlinear interaction of air with vibrating parts of the setup, being especially apparent when the amplitude of the vibrations of various parts of the device are different [21]. It does not apply here because the whole seismic mass of the setup moves as one, unless vibrating wire segments or casings are considered.

6. *Radiometer Effects*

This effect arises from the differential heating of parts of the device being tested so that reflected molecules of air acquire more momentum in some locations than in others. In this case, heat evolves

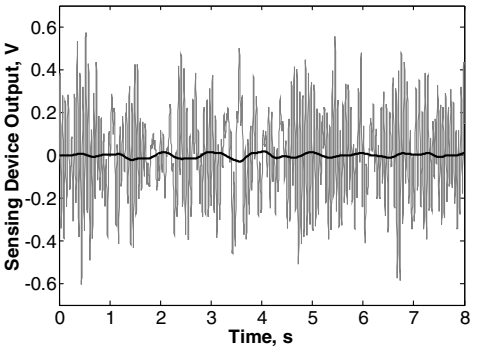

Fig. 8 "Thrust OFF" raw (gray) and filtered (black) experimental data.

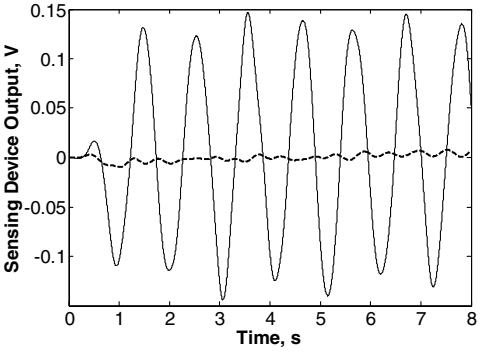

Fig. 9 "Thrust ON" free (solid) and fastened (dotted) blade upper end experimental data.

in the PPU radiators and in the EMMG coils but these effects can be excluded as a contribution to the observed signal because they do not have the right signature. As a temperature induced effect, given the involved heat capacities, it is a smoothly cumulative one, so it cannot account for 1 Hz vibration frequencies.

7. Ground Motion

Ground motion contributes to the observed signal by means of the resulting inertial forces acting upon the sensing device seismic mass. This device being essentially a fourth-order mechanical filter, that contribution consists of a colored noise mostly centered around the two main structure vibration modes, as can be seen in Fig. 6 for the "Open System" setup configuration: 4.5 and 18 Hz. The 50 Hz component is instead of electrical origin corresponding to the ac network frequency going into the measurement lines by imperfect shielding. As mentioned, the ground motion noise at 1 Hz is considerably lower for the actual "Closed System" setup than for any of the previously used setups. Typical levels are shown in Fig. 8 where raw and numerically filtered data, as mentioned at the beginning of this section, are plotted vs time for the thruster in OFF condition. These levels correspond to quiet acoustic-seismic environment (no walking around, nearby city traffic, wind, etc.). They look somehow higher than raw data in Fig. 7 because the tests were performed at different moments of the day. Several runs under such environmental constraints produce, after filtering, an enlarged set of data with zero mean value and $\sigma = 0.007$ V. The ground motion influence at 1 Hz can thus conservatively be estimated to lie within the ± 0.02 V band.

8. Power Supply Induced EMI

Power supply induced electromagnetic interference (EMI) on the measurement channels, sharing the same spectral signature with the pursued effect, has been deemed an issue in former test series, where no attempt was done of assessing its influence on the observed results. The obvious 50 Hz EMI example has already been called forth and similar interference was expected to occur as related to modulated thruster input power.

The thrust stand has a built-in feature allowing for the fastening of the normally free upper end of the resonant blade for safety and transport purposes. Transverse displacements can thus be limited, not rotations. If these "brakes" are used during "Thruster ON" runs, when the modulated power is fully in action, a drastic reduction of the signal is observed, as compared with the same "Thruster ON" runs when the brakes are not applied. Results of filtered data shown in Fig. 9 are considered as a practical proof that this effect amounts to less than 5% of the observed signal.

9. Geomagnetic Influence

By modulating the voltage supply at a frequency different from the carrier frequency, so the seismic setup is excited at the modulation frequency if the proposed formulation is correct, the geomagnetic influence becomes averaged out in the "Open System" setup configuration; the same cannot be said regarding "Closed System" configurations. In fact, in these cases, the force-producing device is self-contained, with all its components, including batteries, sitting in the suspended frame of the sensing fixture. Because the PPU output voltage is required to be modulated, current from the batteries will accordingly be modulated around an almost constant value without sign reversing. As a result, a coupling with the Earth's magnetic field should be expected and because there are no external parts of the circuit, the interaction develops through closed current loops, which applies torques on the fixture.

The PZT-based sensing mechanism is also sensitive to torques. These can be mistaken as forces acting upon the free end of the cantilever beam, if some discriminating procedure is not applied. An important feature to be taken into account is that the sensing mechanism is only sensitive to the component of the torque that lies transversally in the plane of the blade. This means that the significant components of the geomagnetic field with respect to the blade are the vertical (longitudinal) and the perpendicular ones; they are related to the vertical (parallel to the blade's plane) and the horizontal projections of the current loop, respectively.

It is easy to see that, for a given PPU orientation with respect to the blade, the torque due to the vertical projection is a built-in property of the setup, not depending on the thrust stand azimuth angle. Instead, the torque due to the horizontal projection does show a cosine dependence on that angle. Therefore, by performing tests at various azimuth angles, the influence of that torque contribution can be complete and quantitatively assessed. To investigate other spurious influences as mentioned, tests were devised with the PPU operating at nominal conditions, though powering an EMMG electrical emulator, instead of the thruster itself. The emulator consists of a resistor–inductor–capacitor (RLC) circuit electrically equivalent to the EMMG (same input impedance) and is connected to the PPU by means of feeds in practically the same geometrical configuration. A ground reference frame was also adopted with the horizontal axes parallel to the room walls: X_G-axis pointing 10 deg east of magnetic north; Y_G-axis pointing eastward, and Z_G-axis pointing to ground. A local reference frame was ascribed to the thrust stand: X_T-axis along the EMMG longitudinal axis; Z_T-axis along the longitudinal axis of the blade, pointing toward its clamped end; Y_T forming a direct orthogonal frame with the other two axes. Mean amplitudes and 1σ errors obtained for different thrust stand orientations are shown in Table 1.

The response mean values closely agree with a $\cos\psi$ dependence. In spite of lacking intermediate values, two important features arise from these figures: 1) They do not vanish at 90 and 270 deg, as one should expect if the geomagnetic field horizontal (perpendicular to the blade) component were the only acting effect. There is a 0.14 V offset which, in principle, could be ascribed to the vertical

Table 1 PPU ON, EMMG OFF sensing device response, V

Test at			
$\psi = 0$ deg	$\psi = 90$ deg	$\psi = 180$ deg	$\psi = 270$ deg
0.17 ± 0.009	0.136 ± 0.006	0.11 ± 0.005	0.134 ± 0.007

Table 2 PPU ON, EMMG OFF sensing device response with reversed PPU orientation, V

Test at			
$\psi = 0$ deg	$\psi = 90$ deg	$\psi = 180$ deg	$\psi = 270$ deg
0.11 ± 0.006	0.053 ± 0.004	N/A	N/A

Table 3 PPU ON, EMMG ON sensing device response, V

Test at			
$\psi = 0$ deg	$\psi = 90$ deg	$\psi = 180$ deg	$\psi = 270$ deg
0.21 ± 0.01	0.26 ± 0.01	0.28 ± 0.008	N/A

component. 2) The peak-to-peak excursion is around 0.06 V, so the contribution of the horizontal component cannot be higher than 0.03 V. To settle the question the PPU orientation was reversed with respect to the EMMG and tests were performed, again using the EMMG emulator. The results are shown in Table 2.

Combining the results of Tables 1 and 2, consistent values for the horizontal and vertical component contributions can be found provided an additional, nongeomagnetic, effect is taken into account. Both the horizontal and vertical components contribute to around 0.03 V, whereas the residual contribution is around 0.1 V.

It is considered that the observed residual effect is largely due to inner motions related to a transformer ferrite made casing in the PPU's secondary circuit, with minor contribution from eventual electrostatic and magnetic couplings to surroundings, self-magnetic interactions involving loose wiring and, within a negligible extent, to air motion. These residual effects are also expected to appear during testing under "PPU ON–EMMG ON" conditions.

10. Thermal Expansion due to Joule Heating

Thermal expansion of wires subjected to Joule heating during operation is likely to have an impact on the mechanical behavior of the setup, mainly by shifts of centers of mass and changes of moments of inertia of various components. The formers were investigated for configurational asymmetries involving components that could undergo thermal expansion effects. A roughly half loop of the main power wire, 0.4 m length, 1.5-mm-diam, and one of the toroidal coils, 0.15 kg, 25 mm width, were identified as the more significant off-centered candidates. The propulsive effect being detected through oscillatory motion of the overall seismic mass as subjected to a modulated thrust with the input of 15 Wrms modulated power, only harmonic temperature excursions were taken into account sharing the thrust/power modulation frequency. Rough but very conservative estimates show that their contribution to the observed results is at least two orders of magnitude lower than the purported effect. As for changes of moments of inertia due to 30°C of total temperature change during operation, its influence on the first and second natural frequencies of the seismic fixture is well under the PPU tuning accuracy at 1 Hz, i.e., it is less than 0.01 Hz.

11. EMIM Thrusting Results

Tests with activation of the EMMG were performed at various azimuth angles as under the preceding subheading, keeping the nominal PPU orientation. The obtained results are shown in Table 3, as mean and 1σ error values.

The response mean values fairly agree with a $\cos\psi$ law, but they are considerably higher than those obtained during the emulator tests. There is indeed a new effect that adds up to that previously investigated. Because amplitudes of vibration are involved in this study, by comparing the results of Tables 1 and 3, it seems that this new effect has either a $\cos\psi$ dependence with respect to the geomagnetic field or is nearly constant (0.39 ± 0.02 V). In both situations the 0.1 V residual effect simply cancels out if induced by PPU circuitry and components. A constant value is entirely consistent with thrust being produced by the EMMG, depending only on the power delivered by the PPU, which was kept fixed at 200 V on EMMG's capacitors and coils. The claim here is that the new observed results correspond to a genuine electromagnetic inertia manipulation propulsive effect. Thrust stand simulations according to a model presented elsewhere [20] yield a sensing device mean response amplitude of 0.38 V after 20 s of EMMG activation, including microseismic (ground motion) excitation, which accounts for ± 0.01 V peak values 1σ dispersion.

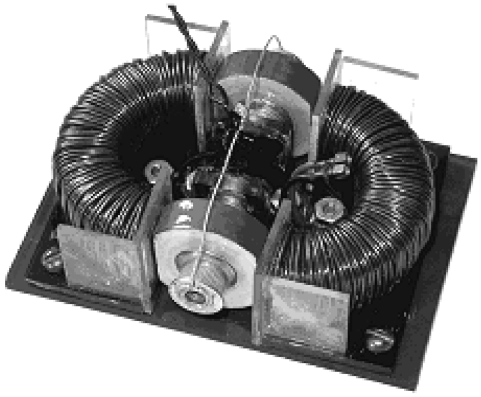

Fig. 10 Woodward's "Mach 3" device (Courtesy of J. Woodward).

V. Woodward's Device

An independent confirmation of the existence of "anomalous" thrusts has recently been produced by J. Woodward using a slightly different device, although conceptually identical to the authors' EMMG [12]. The device (Fig. 10) is made with two modified 5.5 nF high voltage capacitors mounted between two halves of a powdered iron toroidal inductor core, each wound with several hundred turns of bifilar copper magnet wire, so that crossed EM fields develop inside the dielectric. All parts are firmly affixed to a plastic plate and the device is mounted in a Faraday cage with bolts that screw into the outer lugs on the capacitors. Capacitors and inductors were independently ac driven at 50 kHz, yielding about 1 kV peak on each of the capacitors and 4 A peak in the inductor windings. Processed experimental data show that there is little or no thrust present in either the 0 or 180 deg phase settings, as expected. This is not true for the 90 and 270 deg data. A thrust in the range 200–300 μN is present in both cases and the direction of the thrust changes between 90 and 270 deg of phase: exactly as one would expect using Eq. (11) [26].

Precautions were taken to avoid spurious signals as a consequence of switching on the capacitors or due to leakage fields not fully trapped by the Faraday cage. The fact that practically no thrust is present at 0 and 180 deg speaks against the first possibility, whereas the absence of any effects when only one of the two power circuits is activated rules out the second one. Woodward interprets these results in terms of transient mass modifications, strongly relying upon a gravitational radiation reaction as derived from the Mach principle, which seemingly is applied wrongly because masses in General Relativity are not supposed to radiate in a dipolar mode.

VI. Conclusions

The possibility of achieving thrust without reaction mass or beamed power, by means of EM inertia manipulation, has been reviewed. Experimental confirmation of this theoretical concept was sought after and instrumented around a so-called EMIM force-producing device. Tests performed during an exploratory phase produced results, which after intensive data processing gave indirect evidence of matter–electromagnetic field momentum exchange, as predicted by Minkowski's formalism; direct detection of the sought effect could not be achieved due to interfering effects leading to very low S/N ratios. Sustained thrust experiments based on an alternative formulation of the EM force densities were devised and performed, aiming at getting rid of most of the identified spurious effects. They yield sharp and clear evidence of force-producing effects as predicted

by that formulation, albeit in contradiction with null results predicted by the standard formulation.

New experimental results where increased power and sine modulated voltage at a frequency close to the fundamental frequency of the sensing fixture have been applied, allowed to confirm previous results with the alleged propulsive effect showing up well over the ground induced noise. Self-magnetic interactions in wiring and windings of the PPU's components having been identified as an important source of mechanical noise; their influence has been estimated and experimentally assessed as being a minor part of the observed effect. Furthermore, power supply induced EMI on the measurement channels, sharing the same spectral signature with the pursued effect, if present was found to contribute to less than 5% of the observed effect. Other sources of uncertainties have been identified and deemed negligible for all practical purposes. Some uncertainties remain as related to PZT's compression mode sensitivity to inner motions, which might behave differently in thrusting and emulator tests, and unidentified inner motions, which might not eventually show up during EMMG emulator tests. The former are expected to be overcome by means of laser Doppler vibrometry techniques whereas the latter would require a complete redesign of the thruster. Definite answers will have to wait until in-orbit testing could be performed, simultaneously getting rid of all kind of interferences. Present and previous thrust results seem to closely fit theoretical predictions based upon the inclusion of the polarization currents in Lorentz force calculations. J. Woodward's team has recently produced an independent confirmation of the EMIM effect. It has used a slightly different device, albeit conceptually identical to what is proposed here. The observed effects are quantitatively higher than those reported until now by the authors, due to higher power levels fed into the caps-coils arrangement. If this anomalous thrusting effect still persists, propellantless propulsion would have been achieved but additional theoretical work will be needed for full understanding of the underlying physical principles.

Acknowledgments

The author wishes to thank the U.S. Air Force Research Laboratory for supporting the presentation of this work under its Windows-on-Science Program, Grant FA8655-03-1-2A21, and to NASA BPP Project for procuring that help. Supports from the Argentine National Agency for the Advancement of Science and Technology (ANPCyT), Grant FONCyT—PICT-2002-10-10592, and "Instituto Universitario Aeronautico" of Cordoba, Argentina, are also gratefully acknowledged. Work by S. Elaskar was partially supported by Asociacion de Investigaciones Tecnologicas (AIT). We would also like to thank one of the reviewers for bringing our attention to thermal expansion induced mechanical effects as an additional source of uncertainties.

References

[1] Clarke, A. C., "Profiles of the Future," *Beyond the Gravity*, Pan Books, London, 1962, pp. 52–64.

[2] Brito, H. H., "A Propulsion-Mass Tensor Coupling in Relativistic Rockets Motion," *Proceedings of the Space Technology Applications International Forum (STAIF-98)*, Pt. 3, Institute for Space and Nuclear Power Studies, Albuquerque, NM, 1998, pp. 1509–1515.

[3] Brito, H. H., "Propellantless Propulsion by Electromagnetic Inertia Manipulation: Theory and Experiment," *AIP Conference Proceedings 458*, American Institute of Physics, New York, 1999, pp. 994–1004.

[4] Brevik, I., "Definition of Some Energy-Momentum Tensors," *Experiments in Phenomenological Electrodynamics and the Electromagnetic Energy-Momentum Tensor*, Physics Report (Review Section of Physics Letters) Vol. 52, No. 3, North Holland Publishing Co., Amsterdam, 1979, p. 139.

[5] Antoci, S., and Mihich, L., "A Forgotten Argument by Gordon Uniquely Selects Abraham's Tensor as the Energy-Momentum Tensor for the Electromagnetic Field in Homogeneous, Isotropic Matter," *Nuovo Cimento [Sezione] B*, Vol. 112B, No. 7, 1997, pp. 991–1007.

[6] Johnson, F. S., Cragin, B. L., and Hodges, R. R., "Electromagnetic Momentum Density and the Poynting Vector in Static Fields," *American Journal of Physics*, Vol. 62, No. 1, 1994, pp. 33–41.

[7] Jackson, J. D., "Time-Varying Fields, Maxwell's Equations, Conservation Laws," *Classical Electrodynamics*, 2nd ed., John Wiley & Sons, New York, 1962, pp. 169–202.

[8] Portis, A. M., "Fuentes del Campo Electromagnético III—Cantidad de Movimiento del Campo," *Campos Electro-magnéticos*, Special ed., Vol. 2, Ed. Reverté, Barcelona, 1985, pp. 469–472.

[9] Eu, B. C., "Statistical Foundation of the Minkowski Tensor for Ponderable Media," *Physical Review A*, Vol. 33, No. 6, 1986, pp. 4121–4131.

[10] Brito, H. H., "Research on Achieving Thrust by EM Inertia Manipulation," AIAA Paper 2001-3656, July 2001.

[11] Brito, H. H., "Experimental Status of Thrusting by Electromagnetic Inertia Manipulation," *Acta Astronautica*, Vol. 54, No. 8, 2004, pp. 547–558.

[12] Woodward, J. F., "Flux Capacitors and the Origin of Inertia," *Foundations of Physics*, Vol. 34, No. 10, 2004, pp. 1475–1514.

[13] Lai, H. M., "Electromagnetic Momentum in Static Fields and the Abraham-Minkowski Controversy," *American Journal of Physics*, Vol. 48, No. 8, 1980, pp. 658–659.

[14] Brevik, I., "Comment on 'Electromagnetic Momentum in Static Fields and the Abraham-Minkowski Controversy'," *Physics Letters*, Vol. 88A, No. 7, 1982, pp. 335–338.

[15] Lai, H. M., "Reply to 'Comment on "Electromagnetic Momentum in Static Fields and the Abraham-Minkowski Controversy"'," *Physics Letters*, Vol. 100A, No. 4, 1984, p. 177.

[16] Furry, W. H., "Examples of Momentum Distributions in the Electromagnetic Field and in Matter," *American Journal of Physics*, Vol. 37, No. 6, 1969, pp. 621–636.

[17] Walker, G. B., and Walker, G., "Mechanical Forces in a Dielectric due to Electromagnetic Fields," *Canadian Journal of Physics*, Vol. 55, No. 23, 1977, pp. 2121–2127.

[18] James, R. P., "Force on Permeable Matter in Time-Varying Fields," Ph. D. Thesis, Dept. of Electrical Engineering, Stanford Univ., Stanford, CA, 1968.

[19] Obukhov, Y. N., and Hehl, F. W., "Electromagnetic Energy-Momentum and Forces in Matter," *Physics Letters A*, Vol. 311, Nos. 4–5, 2003, pp. 277–284..

[20] Forward, R. L., "Picostrain Measurements with Piezoelectric Transducers," *Journal of Applied Physics*, Vol. 51, No. 11, 1980, pp. 5601–5603.

[21] Brito, H. H., Garay, R., Duelli, R., and Maglione, S., "A Compact, Low-Cost Test Stand for PPT Impulse Bit Measurements," AIAA Paper 2000-3545, July 2000.

[22] Woodward, J. F., and Mahood, T. L., "Mach's Principle, Mass Fluctuations and Rapid Spacetime Transport, " *AIP Conference Proceedings 504*, American Institute of Physics, New York, 2000, pp. 1018–1025.

[23] Cheng, S. I., "Glow Discharge as an Advanced Propulsion Device," *ARS Journal*, Vol. 12, No. 12, 1962, pp. 1910–1916.

[24] Loeb, L. B., "Electric Coronas," *Their Basic Physical Mechanisms*, Univ. of California Press, Berkeley, CA, 1965.

[25] Christensen, E. A., and Moller, P. S., "Ion-Neutral Propulsion in Atmospheric Media," *AIAA Journal*, Vo1. 5, No. 10, 1967, pp. 1768–1773.

[26] Brito, H. H., and Elaskar, S. A., "Overview of Theories and Experiments on Electromagnetic Inertia Manipulation Propulsion," *AIP Conference Proceedings 746*, American Institute of Physics, New York, 2005, pp. 1345–1352.

G. Spanjers
Associate Editor